Zayed *et al. Chemistry Central Journal (2018) 12:26*
https://doi.org/10.1186/s13065-018-0394-5

Chemistry Central Journal

RESEARCH ARTICLE

Open Access

Experimental and theoretical study of donor-π-acceptor compounds based on malononitrile

Mohie E. M. Zayed[1], Reda M. El-Shishtawy[1,2*], Shaaban A. Elroby[1,3], Khalid O. Al-Footy[1] and Zahra M. Al-amshany[1]

Abstract

A set of different donor-π-acceptor compounds having dicyanovinyl as the acceptor and aryl moieties as donors were synthesized by Knoevenagel condensation. The UV–visible absorption and fluorescence spectra were investigated in different solvents. The optical band gab energy (Eg) was linearly correlated with the Hammett resonance effect of the donor to reveal that the higher the value of Hammett resonance effect of a donor, the lower the Eg of the molecule. The photophysical data revealed that compounds M4–M6 are typical molecular rotors with fluorescence due to twisted intramolecular charge transfer. Compound M5 revealed the largest Stokes shift (11,089 cm^{-1}) making it a useful fluorescent sensor for the changes of the microenvironment. The effect of substituents on the optical properties of donor-π-acceptor compounds having dicyanovinyl as the acceptor are studied using density functional theory and time-dependent density functional theory (DFT/TD-DFT). The optical transitions are thoroughly examined to reveal the impact of subtituents on both absorption and fluorescence, mainly through the modification of the structure in the excited state. The theoretical results have shown that TD-DFT calculations, with a hybrid exchange–correlation and the long-range corrected density functional PBEPBE with a 6–311++G** basis set, was reasonably capable of predicting the excitation energies, the absorption and the emission spectra of these molecules.

Keywords: Donor-π-acceptor, Dicyanovinyl, UV–visible and fluorescence spectra, Molecular rotor, DFT, TD-DFT

Introduction

Donor-π-conjugate-electron acceptor (D-π-A) compounds are characterized by having intramolecular charge transfer (ICT) character. These compounds are of great interest owing to their high molar absorptivity [1], amenability of tuning their color by changing the donor, acceptor, and/or π linker [2, 3] and potential applications in optoelectronics [4–6], sensors [7, 8], solvent polarity and others [9]. It is known that cyano group is one of the strongest attracting groups and has been used for the construction of D-π-A dyes [10–20]. On the other hand, dimethylamino group is a strong electron donating group compared with methoxy and/or methyl group.

In this context, we have designed and prepared as series of different benzenoid compounds containing different numbers of methoxy groups, methyl group and dimethylamino group as electron donors compared with the unsubstantiated benzene ring and using dicyanovinyl as the electron acceptor group. It was hypothesized that having acceptor in one side of a conjugated system and connected with different donors on the other side would help understanding the ICT character of such compounds and its impact in their photophysical properties.

In recent years, calculations of electronic structures in the excited states have been a focus of interest because of the development of computations based on Gaussian and the time dependent density functional theory (TDDFT) [21–23]. Also, the solvent effect on the electronic absorption spectra is a useful tool to identify the electronic transitions of the molecules. This would help in studying the chemical properties of the excited states and to

*Correspondence: elshishtawy@hotmail.com; relshishtawy@kau.edu.sa
[1] Chemistry Department, Faculty of Science, King Abdulaziz University, P. O. Box 80203, Jeddah, Saudi Arabia
Full list of author information is available at the end of the article

Springer Open

© The Author(s) 2018. This article is distributed under the terms of the Creative Commons Attribution 4.0 International License (http://creativecommons.org/licenses/by/4.0/), which permits unrestricted use, distribution, and reproduction in any medium, provided you give appropriate credit to the original author(s) and the source, provide a link to the Creative Commons license, and indicate if changes were made. The Creative Commons Public Domain Dedication waiver (http://creativecommons.org/publicdomain/zero/1.0/) applies to the data made available in this article, unless otherwise stated.

distinguish between the different electronic transitions. We will use the Continuum Polarizable model (PCM) [24, 25].

Therefore, computational chemistry is thus necessary to get insight into the molecular structure, although according to our best knowledge no evidence of similar study for the dicyanovinyl effect on the ICT character of the model compounds selected in this study. In this work, interest resides in correlating the theoretically predicted electronic parameters with the accurate experimental results so as to provide possible explanations for the experimentally observed data.

Results and discussion

Synthesis

The compounds (M1, M2, M4–6) were obtained by Knoevenagel condensation in a basic medium as shown in Scheme 1. The structure of these compounds was confirmed by 1H and 13C NMR, mass spectrometry and FTIR.

UV–Visible and fluorescence spectra

Absorption and fluorescence spectra of molecules (M1–6) recorded in $CHCl_3$, CH_3OH and CH_3CN and the photophysical properties of these compounds are shown in Figs. 1, 2, 3, 4, 5, 6 and summarized Table 1, respectively. The molar absorptivity of these compounds indicates that their electronic transition is due to π–π^*. The effect of the donor ability of the substituent groups is nicely correlated with the optical data. Substituting hydrogen atom in compound 1 with different donors shown in Scheme 1 results in a bathochromic shifts in the absorption and in accordance with the donor ability of the substituents.

As the donor groups are in conjunction with acceptor via π-system, thus it was reasonable to correlate the

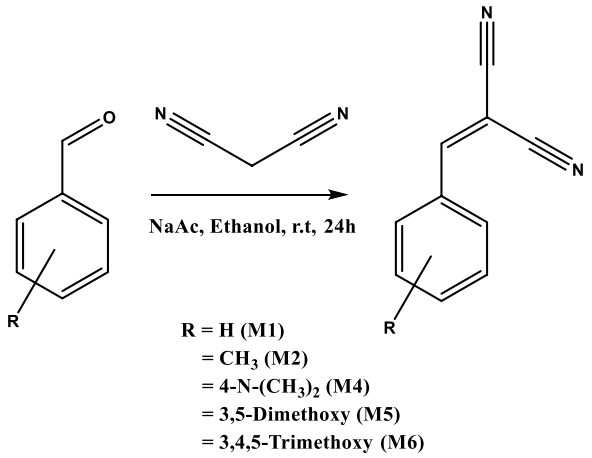

Scheme 1 Synthesis of molecular rotors

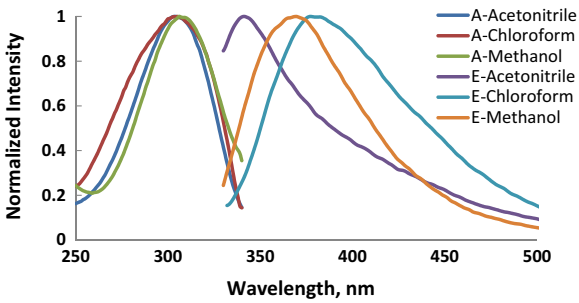

Fig. 1 Normalized absorption (A) and emission (E) spectra of compound M1 (1×10^{-5} M) in different solvents

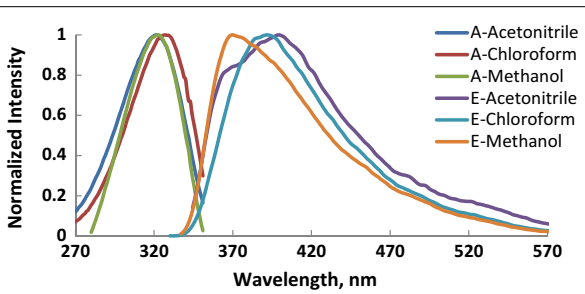

Fig. 2 Normalized absorption (A) and emission (E) spectra of compound M2 (1×10^{-5} M) in different solvents

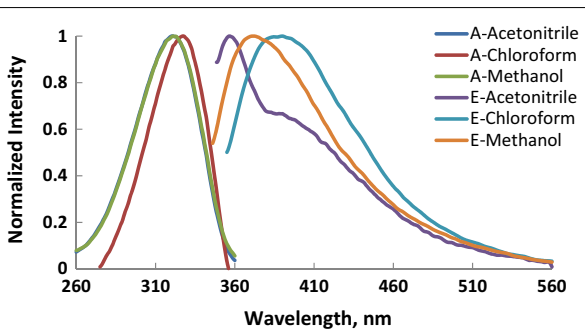

Fig. 3 Normalized absorption (A) and emission (E) spectra of compound M3 (1×10^{-5} M) in different solvents

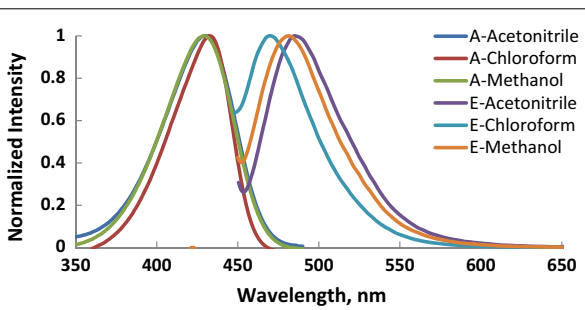

Fig. 4 Normalized absorption (A) and emission (E) spectra of compound M4 (1×10^{-5} M) in different solvents

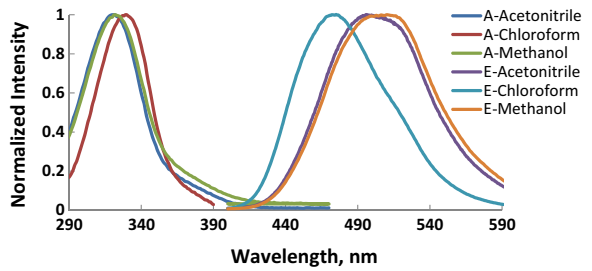

Fig. 5 Normalized absorption (A) and emission (E) spectra of compound M5 (1×10^{-5}M) in different solvents

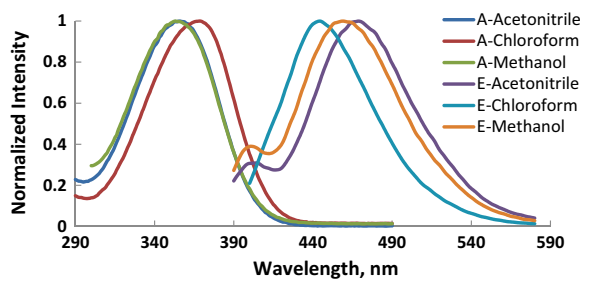

Fig. 6 Normalized absorption (A) and emission (E) spectra of compound M6 (1×10^{-5}M) in different solvents

calculated band gap energy of all compounds with Hammett resonance effect [26]. The optical band gap (E_g) was estimated from the onset wavelength of absorption using the equation of $E_g = 1240/\lambda_{ab}$, onset. Figure 7 shows a linear relation between E_g and Hammett resonance effect of donors. As shown in this figure, the higher the value of Hammett resonance effect of a donor, the lower the E_g of the molecule indicating the involvement of an intramolecular charge transfer (ICT) between donor and acceptor.

Another interesting feature observed in Table 1 and Figs. 1, 2, 3, 4, 5, 6 is the enhanced Stokes shift and bathochromic shift of emission for in different solvents. Correlating the solvents polarity in terms of their dielectric constants with Stokes shifts and emission wavelengths of M4–6 (Fig. 8) gives a direct linear proportion indicating that compounds M4–6 are typical molecular rotors. Molecular rotors are donor-π-acceptor compounds that emit as a result of twisted intramolecular charge transfer (TICT) due to the rotation of donor and/or acceptor in the ground and excited states around sigma bond [27]. This TICT is greatly manifested in compound M5 as evidenced by its relatively higher fluorescence intensity (Fig. 9) as well as its largest Stokes shift (Table 1).

The fluorescent intensity is a function of the free rotation of the molecular rotor and thus a higher fluorescence would be observed dependent on the nature of TICT and/or the fluorophore microenvironment. Since the solvents used are non-viscous solvents thus the huge fluorescence observed in compound M5 compared with other compounds is reflecting its twisted geometry that hampers the free rotation. It is worth noting (Table 1) that compound M5 has the lowest molar absorptivity among all compounds studied indicating a relatively twisted ground state. The very large Stokes shift observed in compound M5 is of practical usefulness as such property would reduce the overlap between the UV–vis absorption and emission spectra of the compound and consequently minimizing the so-called inner filter effect and thus rendering compound M5 as an environment-sensitive fluorescent probe [9, 28–30].

Molecular orbital calculations

The optimized geometries obtained by B3LYP/6-311++G** level of theory for the ground and excited states studied molecules are displayed in Figs. 10 and 11, respectively. DFT calculations give planar optimal geometries for ground and excited states. The characterization of the delocalization of π-electrons along the molecule

Table 1 Photophysical data of compounds M1–6 in different solvents

M	Chloroform				Methanol				Acetonitrile			
	ε, M^{-1} cm^{-1} × 104	λ_{abs}	λ_{em}	Stokes shift, cm^{-1}	ε, M^{-1} cm^{-1} × 104	λ_{abs}	λ_{em}	Stokes shift, cm^{-1}	ε, M^{-1} cm^{-1} × 104	λ_{abs}	λ_{em}	Stokes shift, cm^{-1}
M1	2.35	305	377	6262	3.16	306	370	5653	2.35	304 (324)[a]	341	3569
M2	2.92	327	392	5071	2.20	323	370	3933	2.76	321 (348)	399	6090
M3	3.05	327	390	4940	3.23	321	372	4271	3.06	321 (434)	357	3141
M4	6.02	432	470	1872	5.77	429	481	2520	5.53	430 (403)	485	2637
M5	1.86	329	475	9343	1.86	322	511	11,486	1.92	320 (319)	496	11,089
M6	2.24	369	445	4628	2.16	353	459	6542	2.03	356 (437)	469	6768

[a] Data in brackets are theoretical values using PBEPBE/6–311++G** level of theory in acetonitrile solvent

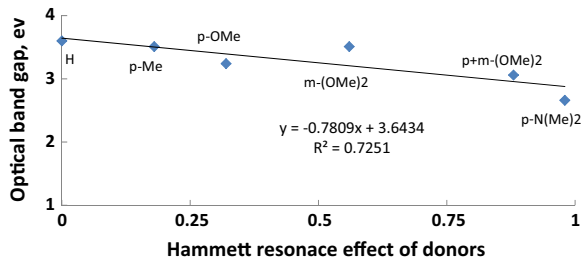

Fig. 7 Hammett resonance effect of donors versus optical band gap of compounds M1–6

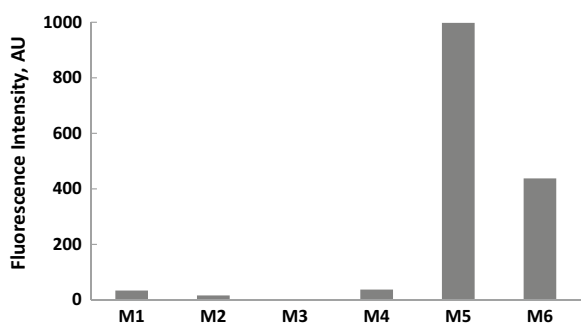

Fig. 9 Relative fluorescence intensity of compounds M1-6 in acetonitrile (1×10^{-5} M)

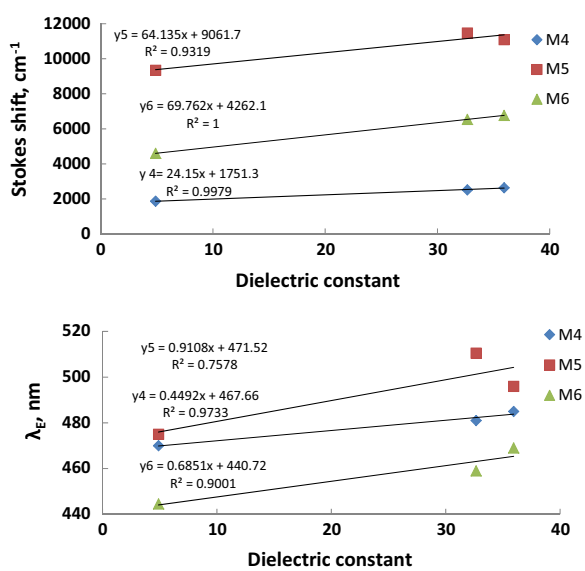

Fig. 8 Solvent polarity versus Stokes shift and emission wavelengths of compounds M4–6

can be estimated by the difference between single and double bond lengths. The small difference between single and double bond lengths corresponds to delocalized charge density on all over the molecules. Table 2 shows the bond lengths and differences between single and double bonds for ground and excited states of the optimal geometries obtained using B3LYP/6-311++G** level of theory. The difference between C–C and C=C in M3 and M5 decrease compared to the other compounds in both ground and excited states. This result indicated that π electron density becomes stronger upon photoexcitation. The bonds between donor and acceptor groups are C8-C1 and C8=C9. The shorter length of these bonds favored the charge transfer (CT) within the studied molecules. Table 2 shows that C8=C9 of M1, M2, M3, M4, M5 and M6 are 1.363, 1.365, 1.372, 1.367, 1.369 and 1.367 Å respectively, while C8-C1 shows more single C–C features. The difference between double and single bond lengths are sorted in the order of M5 > M4 > M6 > M2 > M1, which presents the intensity of interaction between donor and acceptor groups. For all the studied molecules, C8-C1 does not change significantly. The difference between double and single bond lengths are significantly decreased for the excited state (S1) compared to those in the ground state (S_0), especially in M3 and M5 molecules. These results indicate that the connection between acceptor group and donor group for highly enhanced ICT character, which is important for the absorption spectra red-shift.

Absorption spectra

The vertical excited first three singlet states, transitions energies, and oscillator strength using TD-DFT (PBE-PBE) method started from the optimized structures have been calculated. The corresponding simulated UV–visible absorption spectra of all molecules in the gas phase using PBEPBE/6-311++G** level of theory displays in Fig. 12. Table 3 reveals the calculated absorption λ_{max} (nm), frontier molecular orbitals contributions and oscillator strength (f) of the studied compounds (M) collected in Table 3. As shown in Fig. 13 and Table 3, all compounds exhibit a strong absorption band in the region around 450 − 200 nm, which can be assigned to an intramolecular charge transfer (ICT) between the various donating unit and the electron acceptor groups. The λ_{abs} of the studied molecules decreases in the following order M6 > M3 > M5 > M4 > M2 > M1 which is the same order of the band gap except with M3. This bathochromic effect from M1 (304.27 nm) to M3 (397.62) is obviously due to increased π delocalization. With the increasing of conjugation, the λ_{abs} arising from $S_0 \rightarrow S_1$ electronic transition increase. The first excited states for all studied molecules are $\pi \rightarrow \pi*$ transitions which differ in the dominant configuration. The natural transition orbitals (NTO) displayed in Fig. 13, which indicate that all transitions are of $\pi \rightarrow \pi*$ and have a pronounced charge-transfer character.

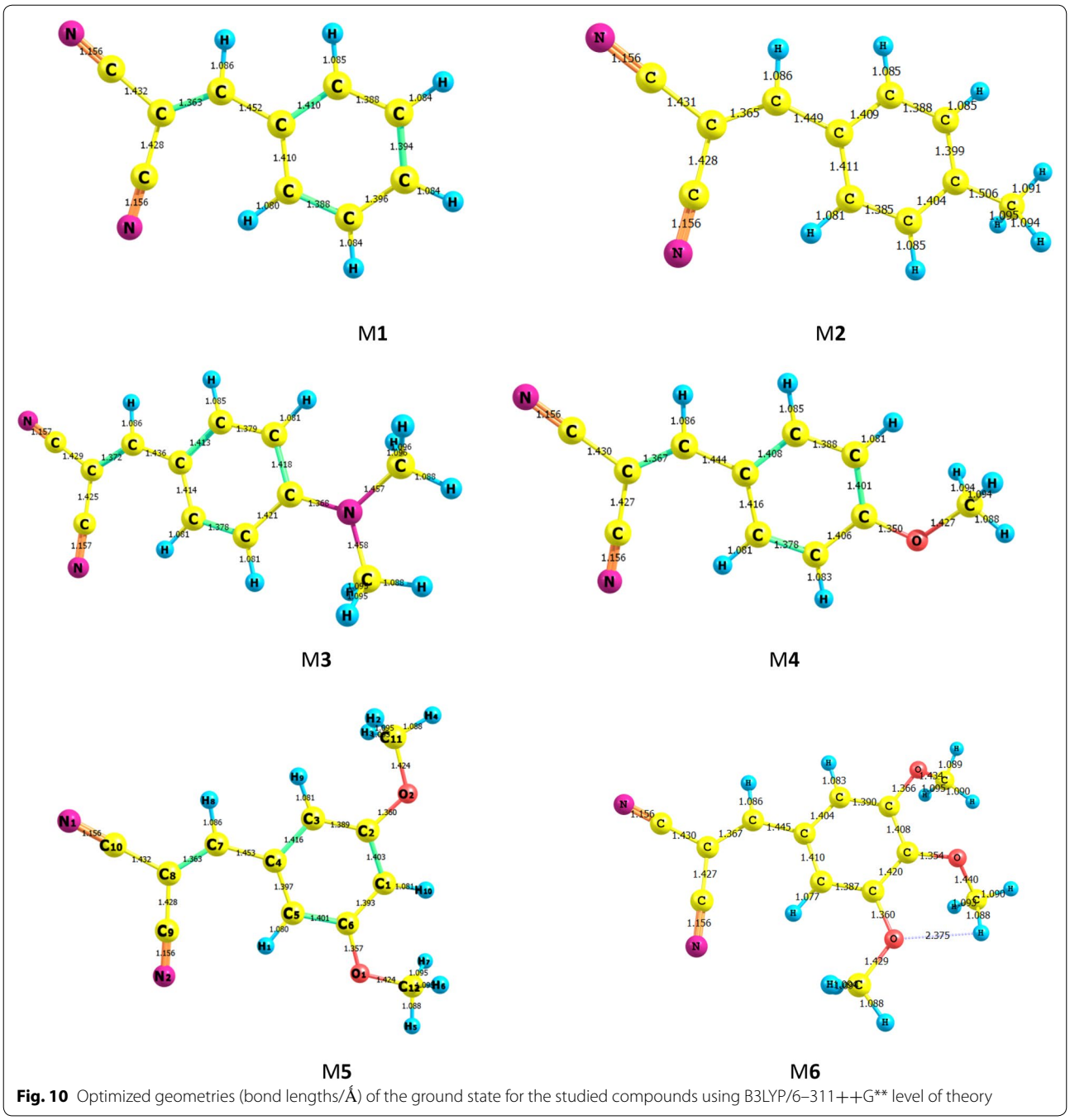

Fig. 10 Optimized geometries (bond lengths/Å) of the ground state for the studied compounds using B3LYP/6–311++G** level of theory

HOMO and LUMO show a pronounced electronic density shift from the donor to the acceptor groups.

Experimental section

General

All solvents and reagents were purchased from Sigma-Aldrich Company and used as received. 2-(4-Methoxybenzylidene)malononitrile (M3) is commercially available at Life Chemicals, Canada and was used as received. 1H and 13C NMR spectra were recorded in $CDCl_3$ solutions on a Bruker Avance 600 MHz spectrometer. Infrared spectra were performed on a PerkinElmer spectrum 100 FTIR spectrometer. Mass spectra were measured on a GCMS-QP1000 EX spectrometer at 70 eV. UV–visible absorption spectra were recorded with a Jasco V560 spectrophotometer (Jasco international Co., Ltd., Tokyo, Japan). Fluorescence spectra were conducted on a Perkin-Elmer LS-55 Luminescence Spectrometer

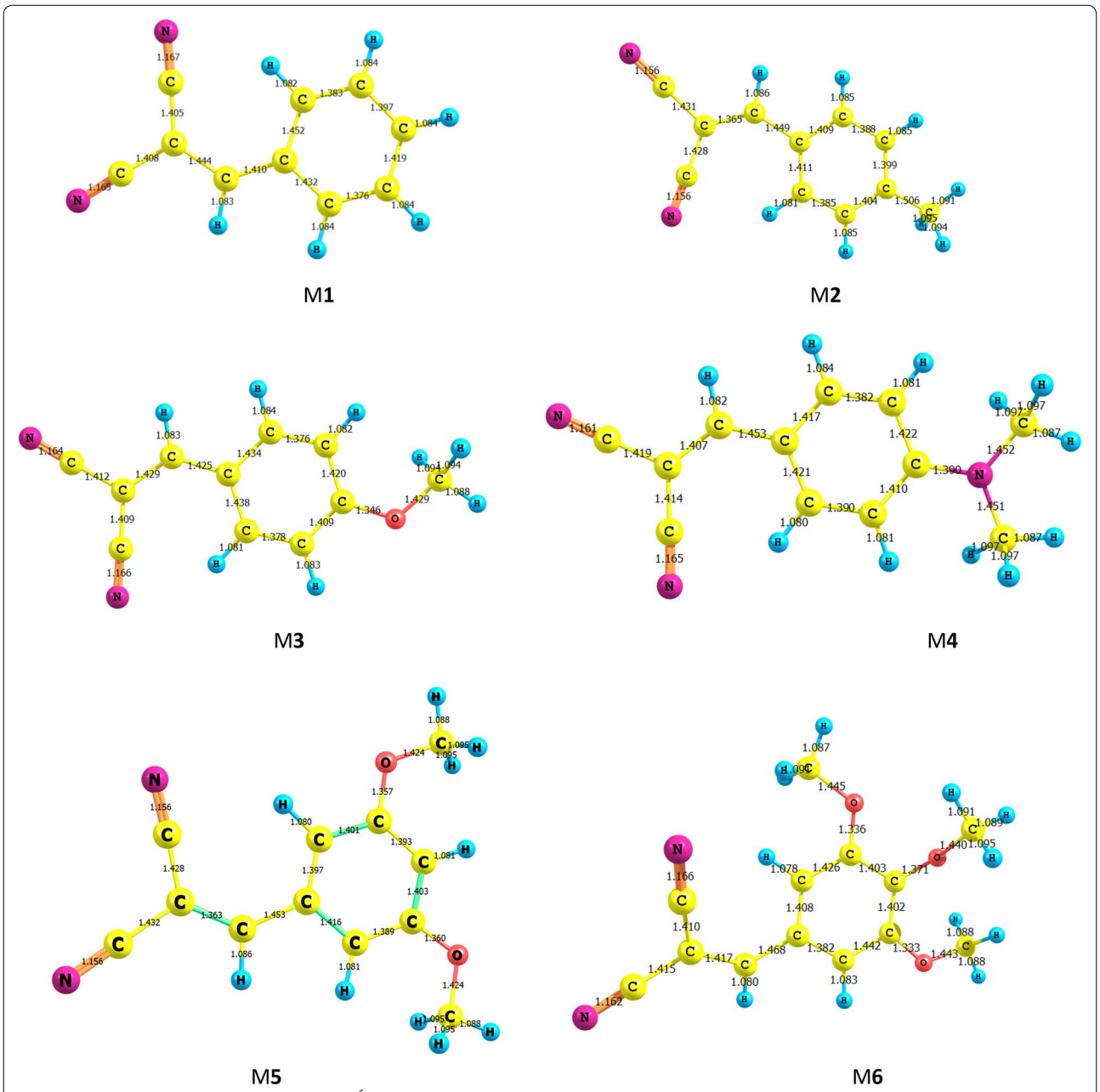

Fig. 11 Optimized geometries (bond lengths/Å) of the excited state for studied compounds using B3LYP/6–311++G** level of theory

and uncorrected. Melting points were determined in open capillary tubes in a Stuart Scientific melting point apparatus SMP3 and are uncorrected.

Synthesis

General procedure

A mixture of aldehyde derivative (10 mmol), malononitrile (10 mmol), sodium acetate anhydrous (12 mmol) and ethanol absolute (30 ml) were stirred at room temperature for 24 h. Then, water was added to the reaction mixture to precipitate the product. The precipitate was filtered, washed water and then dried. Further purification by silica gel column chromatography afforded the corresponding product in good yield.

2-Benzylidenemalononitrile (M1) Solid, m.p:84 °C ^{1}H NMR (600 MHz, $CDCl_3$): ∂ 7.54 (t, 2H, J = 7.2 Hz, Ar–CH), 7.63 (t, 2H, J = 7.2 Hz, Ar–CH), 7.78 (s, 1H, CH=$(CN)_2$),

Table 2 Optimized Selected Bond lengths of the studied molecules obtained by B3LYP/6–311++G level**

M	Ground state			Excited state	
	C4–C8	C8–C9	(4-C9)-(8-C9)	C4-C8	C8-C9
M1	1.452	1.363	0.089	1.410	1.444
M2	1.449	1.365	0.084	1.365	1.449
M3	1.436	1.372	0.064	1.458	1.407
M4	1.444	1.367	0.077	1.425	1.429
M5	1.453	1.363	0.090	1.4507	1.417
M6	1.445	1.367	0.078	1.468	1.417

7.90 (d, 2H, J = 7.2 Hz, Ar–CH). ^{13}C NMR (150 MHz, $CDCl_3$): ∂ 82.88, 112.57, 113.73, 129.67, 130.77, 130.93, 134.69, 159.9; ATR-IR: 3043, 2222, 1589, 1567, 1449; MS (*m/z*) for $C_{10}H_6N_2$ $(M-H)^+$: Calcd: 153.05, Found: 153.

2-(4-Methylbenzylidene)malononitrile (M2) Solid, m.p:135 °C ^{1}H NMR (600 MHz, $CDCl_3$): ∂ 2.45 (s, 3H, CH_3), 7.32 (d, 2H, J = 7.8 Hz, Ar–CH), 7.71 (s, 1H, $CH{=}(CN)_2$), 7.8 (d, 2H, J = 7.8 Hz, Ar–CH). ^{13}C NMR (150 MHz, $CDCl_3$): ∂ 22.05, 81.27, 112.88, 114.04, 128.50, 130.41, 130.95, 146.41, 159.79; ATR-IR: 3035, 2221, 1605, 1584, 1553, 1509; MS (*m/z*) for $C_{11}H_8N_2$ $(M-H)^+$: Calcd: 167.07, Found: 167.

2-(4-(Dimethylamino)benzylidene)malononitrile (M4) Solid, m.p:180 °C ^{1}H NMR (600 MHz, $CDCl_3$): ∂ 3.14 (s, 6H, $N(CH_3)_2$), 6.68 (d, 2H, J = 9 Hz, Ar–CH), 7.46 (s, 1H, $CH{=}(CN)_2$), 7.81 (d, 2H, J = 9 Hz, Ar–CH). ^{13}C NMR (150 MHz, $CDCl_3$): ∂ 40.15, 71.95, 111.60, 114.95, 116.03, 119.31, 133.83, 154.22, 158.16; ATR-IR: 2920, 2207, 1607, 1560, 1515, 1385, 1357; MS (*m/z*) for $C_{12}H_{11}N_3$ $(M-H)^+$: Calcd: 196.1, Found: 196.

Table 3 Absorption wavelength (nm), molecular orbital contribution, energy level of HOMO, LUMO and oscillator strength calculated by using PBEPBE/6–311++G level of theory in gas phase**

M	Wave length (nm)	f	MO contribution	MO coeff. (%)
M1	304	0.542	HOMO–LUMO	94
	297	0.119	HOMO-1-LUMO	91
	179	0.414	HOMO-1-LUMO+1	57
M2	331	0.536	HOMO–LUMO	85
	335	0.15	HOMO-1-LUMO	84
M3	397	0.705	HOMO–LUMO	98
	285	0.216	HOMO-1-LUMO	89
M4	354	0.69	HOMO–LUMO	98
	269	0.147	HOMO-2-LUMO	71
M5	393	0.154	HOMO-1-LUMO	63
	300	0.519	HOMO-2-LUMO	62
M6	434	0.17	HOMO-1-LUMO	96
	413	0.339	HOMO–LUMO	92
	294	0.289	HOMO-3-LUMO	79

2-(3,5-Dimethoxybenzylidene)malononitrile (M5) Solid, m.p:89 °C ^{1}HNMR (600 MHz, $CDCl_3$): ∂ 3.83 (s, 6H, OCH_3), 6.69 (s, 1H, Ar–CH), 7.03 (s, 2H, Ar–CH), 7.68 (s, 1H, $CH{=}(CN)_2$).^{13}C NMR (150 MHz, $CDCl_3$): ∂ 55.71, 83.12, 107.22, 108.24, 112.66, 113.68, 132.35, 160.14, 161.25; ATR-IR: 2966, 2229, 1603, 1577, 1458, 1426, 1310; MS (*m/z*) for $C_{12}H_{10}N_2O_2$ $(M-H)^+$: Calcd: 213.07, Found: 213.

2-(3,4,5-Trimethoxybenzylidene)malononitrile (M6) Solid, m.p:145 °C ^{1}H NMR (600 MHz, $CDCl_3$): ∂ 3.90 (s, 6H, OCH_3), 3.97 (s, 3H, OCH_3), 7.18 (s, 2H, Ar–CH), 7.65 (s, 1H, $CH{=}(CN)_2$).^{13}C NMR (150 MHz, $CDCl_3$): ∂ 56.37, 61.30, 80.60, 108.26, 113.23, 114.02,

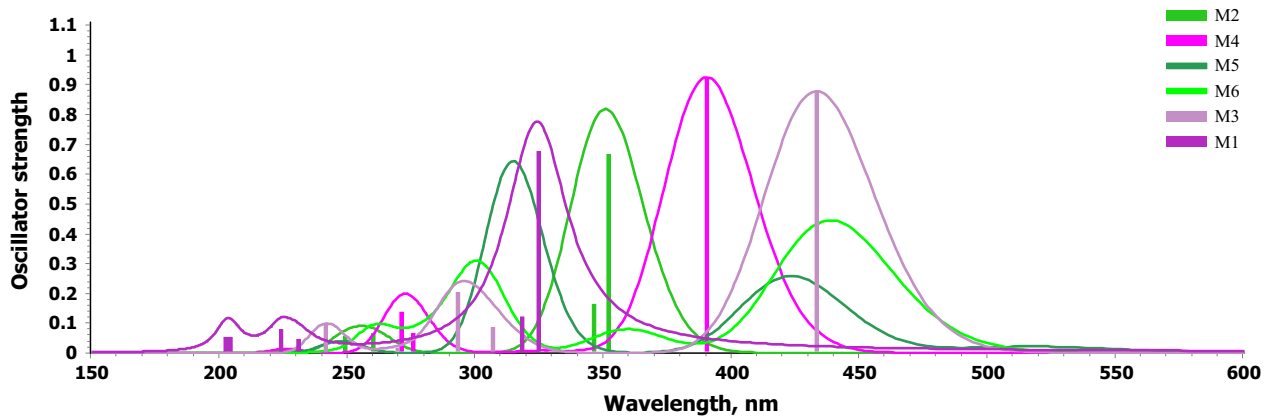

Fig. 12 The UV–visible absorption spectra of the studied compounds calculated using PBEPBE/6–311++G** level of theory in chloroform

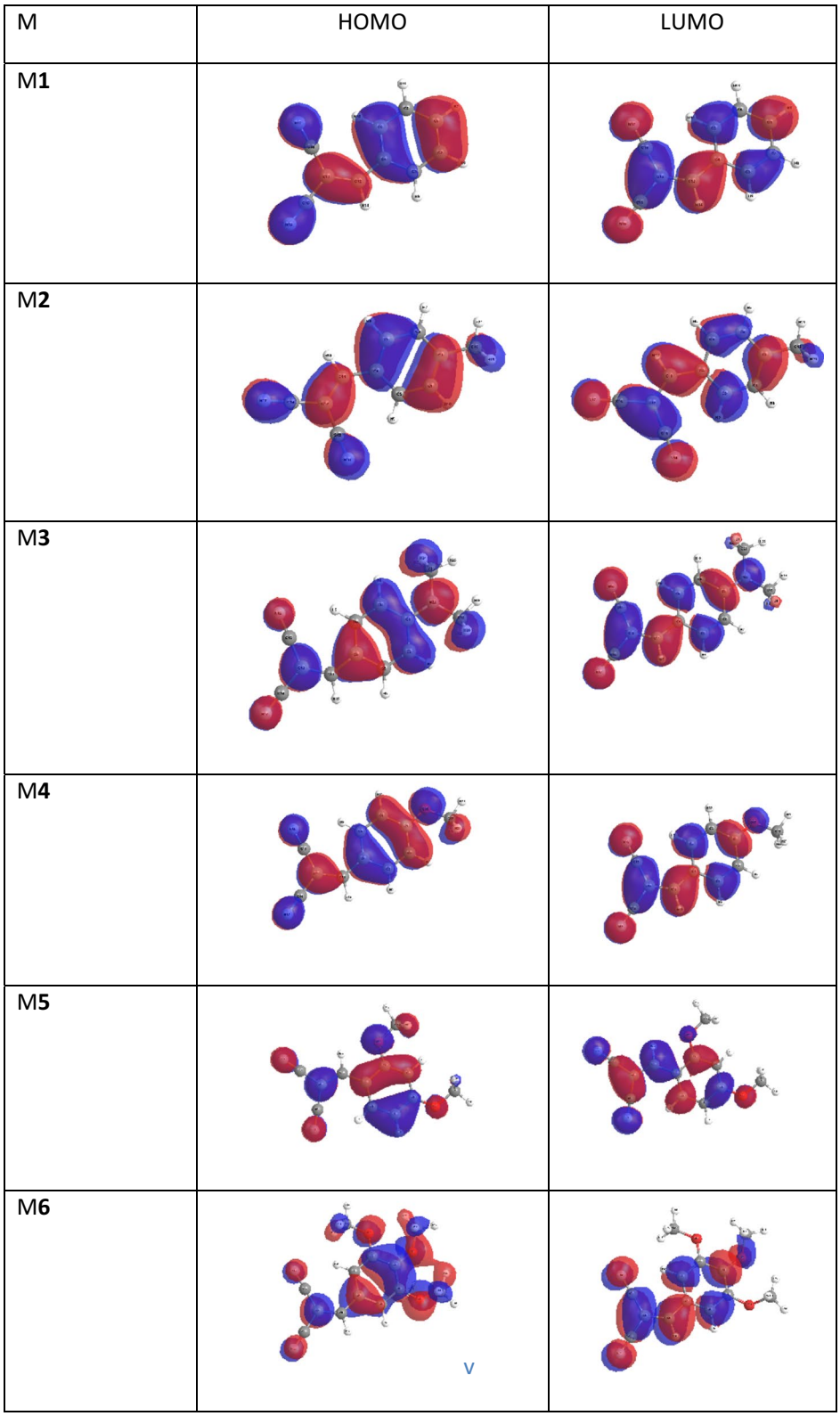

Fig. 13 Schematic diagram of NTO's of four studied dyes calculated at the PBEPBE/6–311++G** level of theory. The surfaces are generated with an isovalue at 0.02

125.96, 143.97, 153.37, 159.45; ATR-IR: 2942, 2839, 2221, 1568, 1499, 1455, 1247, 1126.92; MS (*m/z*) for $C_{13}H_{12}N_2O_3$ $(M-H)^+$: Caled: 243.1, Found: 243.

Computational methods

All calculations are performed using Gaussian 09 W [21] program package. In the present work, B3LYP/6–311++G** level of theory is employed to achieve our aim from this study. Becke's three parameter hybrids function combined with the Lee–Yang–Parr correlation function (B3LYP) [31–34] predict the best results for molecular geometry and electronic transition for moderately larger molecules. B3LYP/6–311++G** frequency analysis calculations were performed to characterize the stationary points as the minima. HOMO–LUMO energies, absorption wavelengths and oscillator strengths are calculated using TD-B3LYP [35–37]. These optimized structures were calculated for the first excitation energy, maximal absorption wavelength (λ_{max}) and oscillator strengths (f) for the three states by using TD-B3LYP/6–311++G** level of theory. Moreover, three density functional, namely, PBEPBE [38] with same above basis set have been evaluated in order to find out the suitable functional that estimates the absorption behavior of the studied dyes.

Conclusions

In this paper, different donor-π-acceptor compounds having dicyanovinyl as the acceptor and aryl moieties as donors were synthesized. Compared with all molecules investigated, molecule 5 showed the highest Stokes shift as well as the highest fluorescent intensity indicating a typical molecular rotor. Also, the energy Eg values were nicely correlated with the donor ability of the substituent as presented by Hammett resonance effect. UV–visible absorption maxima of the compounds were examined experimentally as well as computationally and the results obtained have shown that TD-DFT calculations, with a hybrid exchange–correlation and the long-range corrected density functional PBEPBE with a 6–311++G** basis set, was reasonably capable of predicting the excitation energies, the absorption and the emission spectra of these molecules.

Authors' contributions

RME suggested the research point and did some of the writing up. SAE carried out the theoretical calculations and the writing up of the theoretical part of the manuscript. MEMZ, KOA, and ZMA carried out experimental part (preparation and characterization). All authors shared equally the revision of the manuscript. All authors read and approved the final manuscript.

Author details

[1] Chemistry Department, Faculty of Science, King Abdulaziz University, P. O. Box 80203, Jeddah, Saudi Arabia. [2] Dyeing, Printing and Textile Auxiliaries Department, Textile Research Division, National Research Center, Dokki, Cairo 12622, Egypt. [3] Chemistry Department, Faculty of Science, Beni-Suef University, Beni-Suef 6251, Egypt.

Acknowledgements

This project was funded by the Deanship of Scientific Research (DSR) at King Abdulaziz University, Jeddah, under Grant Number (337/130/1434). The authors, therefore, acknowledge with thanks DSR technical and financial support.

Competing interests

The authors declare no competing interests.

Ethics approval and consent to participate

Not applicable.

Publisher's Note

Springer Nature remains neutral with regard to jurisdictional claims in published maps and institutional affiliations.

Received: 13 December 2017 Accepted: 23 February 2018
Published online: 09 March 2018

References

1. El-Shishtawy RM, Elroby SA, Asiri AM, Müllen K (2016) Optical absorption spectra and electronic properties of symmetric and asymmetric squaraine dyes for use in dssc solar cells: DFT and TD-DFT studies. Int J Mol Sci 17:487–495
2. El-Shishtawy RM, Borbone F, Al-Amshany ZM, Tuzi A, Barsella A, Asiri AM, Roviello A (2013) Thiazole azo dyes with lateral donor branch: synthesis, structure and second order NLO properties. Dyes Pigments 96:45–51
3. Lu H, Mack J, Yang Y, Shen Z (2014) Structural modification strategies for the rational design of red/NIR region BODIPYs. Chem Soc Rev 43:4778–4823
4. El-Shishtawy RM (2009) Functional dyes, and some hi-tech applications. Int J Photoenergy 2009:21
5. Ji C, Yin L, Li K, Wang L, Jiang X, Suna Y, Yanqin L (2015) D–π–A–π–D-type low band gap diketopyrrolopyrrole based small molecules containing an ethynyl-linkage: synthesis and photovoltaic properties. RSC Adv 5:31606–31614
6. El-Shishtawy RM, Al-Zahrani FAM, Afzal SM, Razvi MAN, Al-Mashany ZM, Bakry AH, Asiri AM (2016) Synthesis, linear and nonlinear optical properties of a new dimethine cyanine dye derived from phenothiazine. RSC Adv 6:91546–91556
7. El-Shishtawy RM, Al-Zahrani FAM, Al-amshany ZM, Asiri AM (2017) Synthesis of a new fluorescent cyanide chemosensor based on phenothiazine derivative. Sens Actuators B 240:288–296
8. Beer PD, Gale PA (2001) Anion recognition and sensing: the state of the art and future perspectives. Angew Chem Int Ed 40:486–516
9. Grabowski ZR, Rotkiewicz K, Rettig W (2003) Structural changes accompanying intramolecular electron transfer: focus on twisted intramolecular charge-transfer states and structures. Chem Rev 103:3899–4032
10. Yanga Y, Li B, Zhang L (2013) Design and synthesis of triphenylamine-malonitrile derivatives as solvatochromic fluorescent dyes. Sens Actuators B 183:46–51 **(and references cited therein)**
11. Li X, Kim SH, Son YA (2009) Optical properties of donor-π-(acceptor) n merocyanine dyes with dicyanovinylindane as acceptor group and triphenylamine as donor unit. Dyes Pigments 82:293–298
12. Kim SH, Gwon SY, Bae JS, Son YA (2011) The synthesis and spectral properties of a stimuli-responsive D-π-A charge transfer dye. Spectrochim Acta Part A 78:234–237
13. Son YA, Gwon SY, Lee SY, Kim SH (2010) Synthesis and property of solvatochromic fluorophore based on D-π-A molecular system: 2-{[3-Cyano-4-(N-ethyl-N-(2-hydroxyethyl)amino)styryl]-5,5-dimethylfuran-2(5H)-ylidene}malononitrile dye. Spectrochim Acta Part A 75:225–229
14. Li Y, Ren T, Dong W-J (2013) Tuning photophysical properties of triphenylamine and aromatic cyano conjugate-based wavelength-shifting

compounds by manipulating intramolecular charge transfer strength. J Photochem Photobiol A Chem 251:1–9
15. Bolduc A, Dong Y, Guérinz A, Skene WG (2012) Solvatochromic investigation of highly fluorescent 2-aminobithiophene derivatives. Phys Chem Chem Phys 14:6946–6956
16. Giordano L, Shvadchak VV, Fauerbach JA, Jares-Erijman EA, Jovin TM (2012) Highly solvatochromic 7-aryl-3-hydroxychromones. J Phys Chem Lett 3:1011–1016
17. Hofmann K, Spange S (2012) Influence of the boron atom on the solvatochromic properties of 4-nitroaniline-functionalized boronate esters. J Org Chem 77:5049–5055
18. Kucherak OA, Richert L, Mély Y, Klymchenko AS (2012) Dipolar 3-methoxychromones as bright and highly solvatochromic fluorescent dyes. Phys Chem Chem Phys 14:2292–2300
19. Benedetti E, Kocsis LS, Brummond KM (2012) Synthesis and photophysical properties of a series of cyclopenta[b]naphthalene solvatochromic fluorophores. J Am Chem Soc 134:12418–12421
20. Huang GJ, Ho JH, Prabhakar C, Liu YH, Peng SM, Yang JM (2012) Site-selective hydrogen-bonding-induced fluorescence quenching of highly solvatofluorochromic GFP-like chromophores. Organic Letters 14:5034–5037
21. Frisch MJ, Trucks GW, Schlegel HB, Scuseria GE, Robb MA, Cheeseman JR, Scalmani G, Barone V, Mennucci B, Petersson GA et al (2009) Gaussian 09 Suite of Programs. Gaussian Inc, Wallingford
22. Burke K, Werschnik J, Gross EKU (2005) Time-dependent density functional theory: past, present, and future. J Chem Phys 123:062206
23. Foreman JB, Head-Gordon M, Pople JA (1992) Toward a systematic molecular orbital theory for excited states. J Phys Chem 96:135
24. Miertus S, Scrocco E, Tomasi J (1981) Electrostatic interaction of a solute with a continuum. A direct utilizaion of AB initio molecular potentials for the prevision of solvent effects. Chem Phys 55:117–129
25. Miertus S, Tomasi J (1982) Approximate evaluations of the electrostatic free energy and internal energy changes in solution processes. Chem Phys 65:239
26. Hansch C, Leo A, Taft RW (1991) A survey of Hammett substituent constants and resonance and field parameters. Chem Rev 91(2):165–195
27. Haidekker MA, Theodorakis EA (2010) Environment-sensitive behavior of fluorescent molecular rotors. J Biol Eng 4:11
28. Liu X, Xu Z, Cole JM (2013) Molecular design of uv–vis absorption and emission properties in organic fluorophores: toward larger bathochromic shifts, enhanced molar extinction coefficients, and greater stokes shifts. J Phys Chem C 117:16584–16595
29. Haidekker MA, Theodorakis EA (2007) Molecular rotors–fluorescent biosensors for viscosity and flow Org. Biomol Chem 5:1669–1678
30. Demchenko P, Mely Y, Duportail G, Klymchenko AS (2009) Monitoring biophysical properties of lipid membranes by environment-sensitive fluorescent probes. Biophys J 96:3461–3470
31. Becke AD (1993) Density-functional thermochemistry. III. The role of exact exchange. J Chem Phys 98:5648
32. Lee C, Yang W, Parr RG (1988) Development of the Colle-Salvetti correlation-energy formula into a functional of the electron density. Phys Rev B 37:785
33. Becke AD (1996) Density-functional thermochemistry. IV. A new dynamical correlation functional and implications for exact-exchange mixing. J Chem Phys 104:1040–1046
34. Becke AD (1997) Density-functional thermochemistry. V. Systematic optimization of exchange-correlation functionals. J Chem Phys 107:8554–8560
35. Perdew JP, Burke K, Ernzerhof M (1996) Generalized gradient approximation made simple. Phys Rev Lett 77:3865–3868
36. Casida ME, Jamorski C, Casida KC, Salahub DR (1998) Molecular excitation energies to high-lying bound states from time-dependent density-functional response theory: characterization and correction of the time-dependent local density approximation ionization threshold. J Chem Phys 108:4439–4449
37. Jacquemin D, Wathelet V, Perpete EA, Adamo C (2009) Extensive TD-DFT benchmark: singlet-excited states of organic molecules. J Chem Theor Comput 5:2420–2435
38. Adamo C, Barone V (1999) Toward reliable density functional methods without adjustable parameters: the PBE0 model. J Chem Phys 110:6158–6170

Submit your manuscript to a SpringerOpen journal and benefit from:

► Convenient online submission
► Rigorous peer review
► Open access: articles freely available online
► High visibility within the field
► Retaining the copyright to your article

Submit your next manuscript at ► springeropen.com